Enhancing the in-plane spatial ordering of quantum dots

W. Q. Ma,* M. L. Hussein, J. L. Shultz, and G. J. Salamo
Department of Physics, University of Arkansas, Fayetteville, Arkansas 72701, USA

T. D. Mishima and M. B. Johnson
Department of Physics & Astronomy, University of Oklahoma, Norman, Oklahoma 73019, USA
(Received 10 November 2003; revised manuscript received 10 February 2004; published 25 June 2004)

We report on the use of (In,Ga)As/GaAs multilayer stacking at elevated growth temperatures to produce enhanced in-plane spatial ordering. Cross-sectional transmission electron microscopy images reveal that the (In,Ga)As islands are vertically correlated while atomic force microscopy images demonstrate lateral ordering of quantum dots that are closely aligned along the $[0\bar{1}1]$ direction as chains which are themselves positioned periodically along the [011] direction. The in-plane spatial ordering along the $[0\bar{1}1]$ and [011] directions is directly seen by asymmetric (311) glancing exit x-ray diffraction with the x-ray beam along the respective direction. Growth studies as a function of temperature indicated that the observed lateral ordering results from enhanced surface diffusion and the vertical transfer of corresponding anisotropic strain pattern due to the anisotropy of surface diffusion.

DOI: 10.1103/PhysRevB.69.233312 PACS number(s): 68.65.Hb, 68.65.Ac, 68.55.−a

The fabrication of quantum dots (QD's) based on the self-assembly of three-dimensional (3D) islands in lattice-mismatched growth is usually characterized by broad size and shape profiles as well as a random spatial distribution. The broadened characteristic features result in a correspondingly inhomogeneously broadened optical emission spectrum that seriously limits potential optoelectronic applications. Likewise, the observed random spatial distribution also limits potential applications, such as the fabrication of photonic crystals. In fact, improvements in both of these areas are needed to make it possible to realize many proposed novel devices.[1]

One approach to improve the uniformity and spatial ordering of QD structures is through the vertical ordering that is achieved by stacking QD layers between barrier spacer layers.[2,3] In this case, if the spacer layer thickness is relatively thin, the strain mediation of buried QD's causes subsequent QD layers to deposit on the locations of the spacer layer where the strain field induces a local minimum of lattice mismatch. With this approach, island uniformity is observed to improve.[3,4]

To improve on lateral ordering, one approach taken is based on selective growth on patterned substrates so that the QD's can nucleate and be positioned at defined locations. Another promising approach has been to deposit QD's on a natural template,[5,6] such as a uniform quantum wire structure[7] or a periodically dislocated buffer layer.[6] More recently, well-defined QD structures demonstrating distinct in-plane spatial ordering have been achieved using only vertical stacking of QD's on a flat surface.[8] In this paper, we clarify the underlying physics responsible for the lateral ordering observed in these layered structures.

For the investigation reported here, two types of samples were grown by solid-source molecular beam epitaxy (MBE) on semi-insulating GaAs (100) substrates. The growth process for the first type of sample, denoted as sample *a*, is as follows. After the desorption of the native oxide at 580 °C under As_4 atmosphere, a 0.5-μm-thick GaAs buffer layer was deposited also at 580 °C with a growth rate of 1.3 ML/sec. The substrate was then cooled down to 540 °C for the growth of a QD superlattice structure. For the growth of the superlattice structure, the growth rate of GaAs was reduced to 0.18 ML/sec. The superlattice consists of 15 periods of an $In_{0.38}Ga_{0.62}As$/GaAs multilayer. The thickness of the (In,Ga)As and GaAs layers in the superlattice was 2.4 and 22 nm, respectively, which were determined by x-ray diffraction (XRD) measurements of the symmetric (400) reflection after the growth. Finally, in order to see the surface morphology, a 2.4-nm-thick (In,Ga)As layer was grown on top of the superlattice. Because the growth temperature is relatively high, following every deposition of the (In,Ga)As layer, three monolayers of GaAs were grown without interruption to suppress In segregation. After 10 sec of growth interruption, the rest of the GaAs layer growth was initiated. The As_4 to Ga beam equivalent pressure (BEP) ratio during the growth was about 15. The growth procedure of the second sample, denoted as sample *b*, was exactly the same as sample *a* except that the growth temperature of the (In,Ga)As/GaAs superlattice was 480 °C instead of 540 °C.

Figures 1(a) and 1(b) show tapping-mode atomic force microscopy (AFM) top views of samples *a* and *b*, respectively. For Fig. 1(a), a distinct in-plane spatial ordering along the [011] and $[0\bar{1}1]$ directions can be seen. It is observed that the QD's are closely arranged along the $[0\bar{1}1]$ direction as chains and the chains are positioned periodically along the [011] direction. The bottom of Fig. 1(a) shows a line scan of the AFM image along the [011] direction corresponding to the position at the top of Fig.1(a) marked as a white line. The AFM image shows that the diameter of the QD's is about 54 nm and the periodicity along the [011] direction is about 110 nm. As a clear comparison, Fig. 1(b) does not reveal in-plane ordering. The size of the QD's grown at 480 °C is about 30 nm, which is smaller than that grown at 540 °C. This is consistent with reported results.[9,10]

 ©2004 The American Physical Society

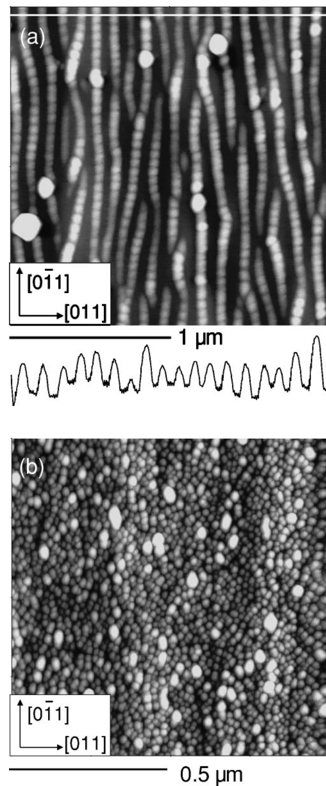

FIG. 1. AFM top views of the samples grown at 540 °C (a) and 480 °C (b). The bottom of (a) shows the line scan corresponding to the position marked as a white line on the top of (a).

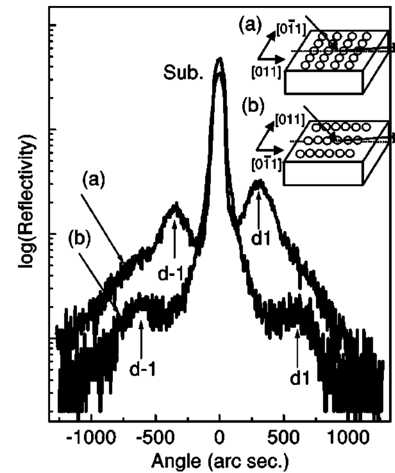

FIG. 2. XRD rocking curves around the asymmetric GaAs (311) glancing exit reflection of the sample grown at 540 °C. (a) and (b) are measured when the scattering plane is along the [011] and [0$\bar{1}$1] directions, respectively. The inset shows the schematic diffraction geometry of (a) and (b). d_{-1} and d_1 denote the −1st and 1st satellites, respectively.

Considering the features observed by AFM, we further employed high-resolution XRD to characterize the two samples. XRD of a periodically surface-corrugated structure can be regarded as a multiple-slit Fraunhofer diffraction.[11] As a result, glancing exit asymmetric diffraction geometry is highly sensitive to the detection of the lateral periodicity.[12] The reason for this increased sensitivity is that the number of coherently diffracted waves that can interfere at the detector is proportional to the square of the asymmetry factor b (Ref. 12). Here b is defined as $b=\gamma_0/\gamma_h$, where γ_0 and γ_h are the direction cosines of the incident and diffracted waves with respect to the inward normal of the sample surface, respectively. Glancing exit (311) diffraction has the largest value of b and therefore is the most sensitive to the lateral periodicity. The measurements were performed by a conventional Philips X'pert double-crystal x-ray diffractometer. The Cu $K\alpha_1$ line is used as the x-ray source, $\lambda=1.54056$ Å, and the monochromator is a Bartels-type four-crystal configuration using the Ge (440) reflection. The step size of the ω scan used in the measurements is 0.001°. Figures 2(a) and 2(b) show the XRD rocking curves of the glancing exit (311) reflection of sample a when the scattering plane contains the [011] and [0$\bar{1}$1] directions, respectively. The inset of Fig. 2 schematically illustrates the diffraction geometry. As shown in Figs. 2(a) and 2(b), two clear satellite peaks are detected due to the lateral periodicity along the [011] and [0$\bar{1}$1] directions, respectively. Here the striking feature is the appearance of the satellites when the x-ray beam is parallel to the [0$\bar{1}$1] direction as shown in Fig. 2(b). The observation of these satellites demonstrates that the QD's within the chains are periodically aligned along the [0$\bar{1}$1] direction while Fig. 2(a) demonstrates that the chains are also positioned periodically along the [011] direction. From the spacing between the satellites, we determine that the average spacing[13] between the chains along the [011] direction—i.e., the lateral period—is 119 nm while the average spacing of the QD's within a chain along the [0$\bar{1}$1] direction is 63 nm. These values are in agreement with those obtained by AFM. Moreover, since the x-ray beam irradiates a large area of the sample and penetrates the total thickness of the superlattice structure, the XRD spectra confirm a high degree of lateral ordering throughout the QD structure. As a comparison, the same XRD measurements were performed for sample b; no satellites were observed, again confirming the absence of in-plane ordering.

Since the glancing exit geometry of XRD measurements is mainly sensitive to the lateral periodicity, we also employed transmission electron microscopy (TEM) to get detailed information on the organization of the buried islands. Figure 3(a) is a cross-sectional TEM image of the whole structure taken along the [0$\bar{1}$1] projection. The dark region corresponds to the (In,Ga)As layer and white region to the GaAs layer. The TEM images support the conclusion that the structure is free of dislocations and the (In,Ga)As islands are vertically correlated from the first layer to the top layer. Figure 3(b) is a magnified cross-sectional TEM image showing the initial seven periods of the structure taken along the [0$\bar{1}$1] projection. It can be seen that, with increasing stacking layers, the (In,Ga)As wetting layer becomes thinner while the (In,Ga)As islands get taller until about the sixth or seventh layer. Beyond the sixth or seventh layer, the wetting layer thickness and the size of the islands are found to sta-

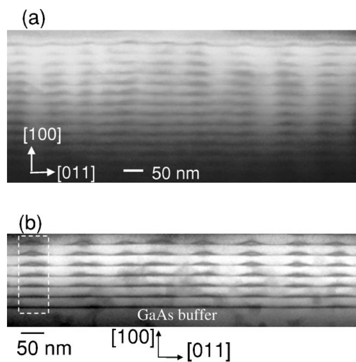

FIG. 3. The cross-sectional TEM images of sample *a* taken along the $[0\bar{1}1]$ projection showing the whole structure (a) and the initial seven periods (b). With increasing the stacking layers, the wetting layer gets thinner and thinner and the QD's get taller and taller as can be seen, for example, from the column marked as the white box.

bilize. Namely, a size ordering of the islands is achieved after about six or seven layers. The vertical correlation of the islands is due to the strain paring between the seeded layer and the subsequent layer.[2] The variation of the island size in the initial several layers is intimately connected to the decrease of the wetting layer thickness. Because the nominal thickness of the (In,Ga)As layer is fixed, a decrease of the wetting layer is consistent with an increased 3D island size. The decrease of the wetting layer is expected due to the increase of the overall strain that accumulates at higher layers while the larger QD size is a result of the lower local lattice mismatch at the 3D nucleation site. Both phenomena have also been observed for Ge/Si multilayered structures[14] and are supported by theoretical calculations.[15]

To explore the mechanism behind the in-plane ordering, the two AFM images are the key. First, the observed differences in the spatial ordering in the two AFM images are consistent with the view that the island formation is a kinetically driven process. Second, based on strain alone, in both cases, a vertical correlation of the islands exists. In fact, the vertical correlation is well documented—for example, Refs. 2 and 16—for growth temperatures between 450 and 500 °C for the (In,Ga)As/GaAs system with a proper choice of spacer layer thickness. Third, consistent with previous reports,[7,10] the (In,Ga)As single layer does not show clear in-plane ordering. Given these observations, it is fair to say that the growth at the elevated temperature of 540 °C generates a greater tendency for lateral ordering for the (In,Ga)As-layered structure compared to that grown at 480 °C. We propose that the origin of the greater lateral ordering tendency at the higher growth temperature arises from the enhanced migration length of adatoms with temperature and that the QD chain formation along the $[0\bar{1}1]$ direction is due to the highly anisotropic surface reconstruction[17] and corresponding diffusion on the GaAs (100) surface. In particular, the diffusion length along the $[0\bar{1}1]$ direction is longer than along the [011] direction. However, as uncovered in some very nice work,[18] islands will preferentially coalesce along the direction where the adatom diffusion is smaller. This seems to be in conflict with our results since the islands in our case are aligned along the dimer rows or the $[0\bar{1}1]$ direction where the material transport or diffusion is higher.[17] However, since the strain can also drive material transport and result in strain relief, the asymmetric transport leads to greater strain relaxation along the $[0\bar{1}1]$ direction, producing an elliptical strain field that is transferred to succeeding layers and is greater along the [011] direction than along the $[0\bar{1}1]$ direction, causing an asymmetric separation between the neighboring dots as observed and as predicted.[3] As can be seen in Fig. 1, the lateral ordering and spacing between dots is indeed highly asymmetric. The point here is that Ref. 18 addresses the growth of submonolayer islands due to island coalescence while our approach to the formation of dot chains relies on the interaction between vertical stacks of dots and the transfer of an anisotropic strain pattern to achieve lateral ordering. These are two very different physical situations. In fact, the self-organization observed in the first layer of our samples is negligible. Moreover, if the spacer layer thickness is large, resulting in vertically noninteracting dot layers, lateral self-organization is not observed in any dot layer. That is, the dot chains are observed only for vertically interacting dot layers.

Finally, we should point out that there is room to improve on the degree of observed spatial ordering. As discussed above, the lateral ordering basically is due to the enhanced adatom migration length that results in an anisotropic strain pattern. Therefore, any factors that can enhance surface diffusion and effectively engineer or control the strain pattern transferred from layer to layer can increase the in-plane spatial ordering. Besides the elevated temperature and low growth rate we employed, these factors could include migration-enhanced epitaxy and a longer growth interruption. We look forward to trying some new ideas in this direction.

In conclusion, we have demonstrated that, for the (In,Ga)As/GaAs multilayer stacking, an elevated growth temperature of 540 °C is effective in producing clear in-plane spatial ordering. Cross-sectional transmission electron microscopy images reveal that the (In,Ga)As islands are vertically correlated and a size ordering occurs after about six- or seven-layer stacking. The atomic force microscopy images show that the (In,Ga)As islands grown at 540 °C are closely aligned along the $[0\bar{1}1]$ direction as chains and the chains are positioned periodically along the [011] direction. The asymmetric (311) glancing exit x-ray diffractions are employed and the lateral ordering is confirmed. Growth studies as a function of temperature have indicated that the observed lateral ordering results from enhanced surface diffusion and, more importantly, the vertical transfer of the corresponding anisotropic strain pattern due to the anisotropy of surface diffusion. The observed lateral ordering should be a universal feature for all similar materials systems. For example, if the adatom migration were large and isotropic, the lateral ordering would still exist, but the surface morphology would not be chainlike.

*Electronic address: wqma@uark.edu

[1] M. S. Miller, Jpn. J. Appl. Phys., Part 1 **36**, 4123 (1997).
[2] Q. Xie, A. Madhukar, P. Chen, and N. Kobayashi, Phys. Rev. Lett. **75**, 2542 (1995).
[3] J. Tersoff, C. Teichert, and M. G. Lagally, Phys. Rev. Lett. **76**, 1675 (1996).
[4] G. Springholz, V. Holý, M. Pinczolits, and G. Bauer, Science **282**, 734 (1998).
[5] T. Mano, R. Nötzel, G. J. Hamhuis, T. J. Eijkemans, and J. H. Wolter, Appl. Phys. Lett. **81**, 1705 (2002).
[6] K. Yamaguchi, K. Kawaguchi, and T. Kanto, Jpn. J. Appl. Phys., Part 2 **41**, L996 (2002).
[7] W. Q. Ma, R. Nötzel, A. Trampert, M. Ramsteiner, H. J. Zhu, H.-P. Schönherr, and K. H. Ploog, Appl. Phys. Lett. **78**, 1297 (2001).
[8] Y. I. Mazur, W. Q. Ma, X. Y. Wang, Z. M. Wang, G. J. Salamo, M. Xiao, T. D. Mishima, and M. B. Johnson, Appl. Phys. Lett. **83**, 987 (2003).
[9] G. S. Solomon, J. A. Trezza, and J. S. Harris, Jr., Appl. Phys. Lett. **66**, 991 (1995).
[10] W. Q. Ma, R. Nötzel, H.-P. Schönherr, and K. H. Ploog, Appl. Phys. Lett. **79**, 4219 (2001).
[11] L. Tapfer, G. C. La Rocca, H. Lage, O. Brandt, D. Heitmann, and K. H. Ploog, Appl. Surf. Sci. **267**, 227 (1992).
[12] L. D. Caro, P. Sciacovelli, and L. Tapfer, Appl. Phys. Lett. **64**, 34 (1994).
[13] A. Krost, G. Bauer, and J. Woitok, in *Optical Characterization of Epitaxial Semiconductor Layers*, edited by G. Bauer and W. Richter (Springer-Verlag, Berlin, 1996), p. 365.
[14] V. L. Thanh, V. Yam, P. Boucaud, F. Fortuna, C. Ulysse, D. Bouchier, L. Vervoort, and J.-M. Lourtioz, Phys. Rev. B **60**, 5851 (1999).
[15] Z.-F. Huang and R. C. Desai, Phys. Rev. B **67**, 075416 (2003).
[16] I. Makhametzhanov, R. Heitz, J. Zeng, and A. Madhukar, Appl. Phys. Lett. **73**, 1841 (1998).
[17] V. P. LaBella, D. W. Bullock, Z. Ding, C. Emery, W. G. Harter, and P. M. Thibado, J. Vac. Sci. Technol. A **18**, 1526 (2000).
[18] M. Meixner, R. Kunert, and E. Schöll, Phys. Rev. B **67**, 195301 (2003).